

EUROPEAN ORGANIZATION FOR NUCLEAR RESEARCH
CERN – ACCELERATOR AND TECHNOLOGY SECTOR

CERN-ATS-2011-093

**SIMULATION STUDIES OF MACROPARTICLES FALLING INTO
THE LHC PROTON BEAM**

N. Fuster Martinez, U. Valencia, Spain; F. Zimmermann, T. Baer, M. Giovannozzi, E.B. Holzer, E. Nebot, A. Nordt, M. Sapinski, CERN, Switzerland; Z. Yang, EPFL Lausanne, Switzerland

Abstract

We report updated simulations on the interaction of macroparticles falling from the top of the vacuum chamber into the circulating LHC proton beam. The path and charge state of micron size micro-particles are computed together with the resulting beam losses, which — if high enough — can lead to the local quench of superconducting (SC) magnets. The simulated time evolution of the beam loss is compared with observations in order to constrain some macroparticle parameters. We also discuss the possibility of a “multiple crossing” by the same macroparticle, the effect of a strong dipole field, and the dependence of peak loss rate and loss duration on beam current and on beam size.



SIMULATION STUDIES OF MACROPARTICLES FALLING INTO THE LHC PROTON BEAM

N. Fuster Martinez, U. Valencia, Spain; F. Zimmermann, T. Baer, M. Giovannozzi, E.B. Holzer, E. Nebot, A. Nordt, M. Sapinski, CERN, Switzerland; Z. Yang, EPFL Lausanne, Switzerland

Abstract

We report updated simulations on the interaction of macroparticles falling from the top of the vacuum chamber into the circulating LHC proton beam. The path and charge state of micron size micro-particles are computed together with the resulting beam losses, which — if high enough — can lead to the local quench of superconducting (SC) magnets. The simulated time evolution of the beam loss is compared with observations in order to constrain some macroparticle parameters. We also discuss the possibility of a “multiple crossing” by the same macroparticle, the effect of a strong dipole field, and the dependence of peak loss rate and loss duration on beam current and on beam size.

INTRODUCTION

In the LHC sudden local spikes with a duration of about 0.1–1.0 ms are routinely observed by the beam-loss monitoring (BLM) system [1, 2, 3]. At a beam energy of 3.5 TeV the location of these fast loss events is distributed rather uniformly around the two LHC rings. They can be found in both cold and warm regions of the machine, and for either beam. At injection energy much fewer of these events are recorded, which could be due to a reduced sensitivity (smaller showers) [2, 3]. However, a few large events have occurred near the injection kickers [3]. The LHC BLM thresholds are set so as to prevent quenches of the cold SC magnets. Occasionally the local loss rate exceeds a BLM threshold and the beam is dumped. Thereby, the fast loss events affect the operational availability of the LHC. The extrapolation to beam energies above 3.5 TeV is a particular concern. It is speculated that these events are caused by macroparticles (e.g. dust or debris) falling into the beam. In the LHC control room they are referred to as UFOs (“unidentified falling objects”).

In an earlier study we have analyzed the motion and charge state of spherical micro-size macroparticles as well as the resulting beam loss rates [4]. There, we could demonstrate that the LHC beam, up to several times the design beam current, cannot pick up any macroparticle lying at the bottom of the metallic vacuum chamber. This conclusion holds for every part of the LHC machine except, possibly, for the injection kickers: The latter represent the only elements where a ceramic chamber wall is in direct sight of the beam, so that the image force may not be present. We also argued, and studied the possibility, that macroparticles could fall into the beam from above, or that they could move towards the beam as a result of mechani-

cal vibration, of eddy currents induced while the magnetic field is ramped (or of an electrical field pulse, e.g. at the kickers).

The simulation results presented in this paper extend those of [4]. In particular, we discuss the dependence of the proton losses on beam current, beam energy or beam size, multiple approaches of the same macroparticle, and the shape of the loss evolution in time.

MACROPARTICLE DYNAMICS

A charged macroparticle moves under the influence of four forces: (1) electric beam force, (2) electric image force, (3) gravity, and (4) magnetic force. Since the heavy macroparticle moves slowly, the bunched nature of the beam is unimportant, and it is sufficient to consider the average electric field of the beam. The magnetic Lorentz force can in first approximation be neglected for the typical speed of the macroparticles despite the high magnetic field $B \approx 8.3$ T of the LHC dipole magnets at top energy [8].

Formulae for the macroparticle acceleration due to the above four forces were presented previously [4], assuming a transversely round beam at the center of a round vacuum chamber, with Gaussian shape and rms size σ (about 300 μ for the LHC at top energy), and a spherical macroparticle with mass A in units of proton masses m_p , density ρ and radius R .

In the following, y denotes the vertical position of a macroparticle with respect to the beam, x its horizontal position, C the circumference of the storage ring (26.7 km for the LHC), N_p the total number of protons in the beam (with the LHC design value of 3.2×10^{14}), c the speed of light, Q the charge of the macroparticle in units of the electron charge, f_{rev} the beam revolution frequency, r_e the classical electron radius, and N_A Avogadro’s number. The radius R of the macroparticle is related to its mass A via $R \approx (3A/(4\pi(\rho/\text{kg}) 1000 N_A))^{1/3}$.

Under some assumptions ($Q \gg 1$) the charging rate is determined by the fraction of high-energy secondary electrons (delta-rays) with energy high enough to escape from the electric potential of the dust particle [5],

$$\dot{Q} \approx -\frac{4\pi}{3} f_{\text{rev}} 1000 N_A r_e \frac{N_p}{2\sigma^2} \frac{R^4}{Q} \left(\frac{\rho}{\text{kg}} \right) e^{-\frac{x^2+y^2}{2\sigma^2}}. \quad (1)$$

The coupled nonlinear equations of motion including (1) are solved using the Mathematica [6] function *NDSolve*.

Local beam losses arise from hard nuclear interactions with the nuclei of the macroparticle. The local loss rate is estimated as $\dot{N}_p =$

$\sigma_{\text{int}} N_p c / (2\pi\sigma^2 C) (A/A_{\text{atom}}) \exp(-(x^2 + y^2)/(2\sigma^2))$, which depends on the macroparticle through its actual transverse position (x, y) , its weight A , its atomic constituents A_{atom} and its nuclear interaction cross section σ_{int} . It can be computed in a second step after the trajectory of the macroparticle has been determined. The loss rate so obtained can be compared with the quench limit for SC magnets. According to FLUKA simulations the latter corresponds to a value of $1-2 \times 10^7$ protons lost per second at top energy (7 TeV) [7].

RESULTS

We consider a macroparticle made from aluminium, for which $A_{\text{atom}} = 27$, $\rho = 2700 \text{ kg/m}^{-3}$, and $\sigma_{\text{int}} = 420 \text{ mbarn}$. Figure 1 shows trajectories for particles of mass $A = 10^{15}$ falling into a beam of rms size 0.3 mm with varying intensity. For a higher beam intensity the particle is repelled faster and is deflected less. A macroparticle that initially is close to $x = 0$, after having been repelled once, may discharge when it hits the top chamber wall, and then fall into the beam a second time. A pertinent study [8] has shown that, in such a case, the resulting time interval between a first and a second loss spike is of order 80 ms, almost independent of beam intensity. This value is close to the typical time distance for a few multiple UFO events observed in 2010. Simulations have also demonstrated that the presence of a magnetic field up to 10 T does not affect this time interval, and neither the relative amplitudes of first and second loss spike [8].

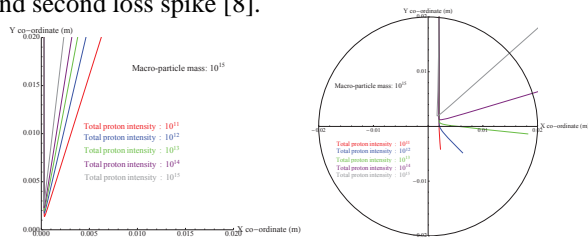


Figure 1: Trajectories in the $x - y$ plane for a macroparticle mass $A = 10^{15}$, an rms beam size 0.3 mm, and varying total proton intensity as indicated. The initial position of the macroparticle was $x_0 = 0.3 \text{ mm}$ (left) and $x_0 = 2 \text{ mm}$ (right).

In the following, we look only at a single approach of macroparticle towards the beam. Figure 2 shows the instantaneous loss rate as a function of time for two different total proton intensities (3.2×10^{13} and 6.5×10^{14} , respectively) and for two rms beam sizes, roughly corresponding to injection energy (1.2 mm) and top energy (0.3 mm). The different curves in each picture represent different particle masses. The loss rate is plotted on a logarithmic scale. Larger macroparticle masses lead to higher loss rates. A longer loss duration for larger beam size and lower beam intensity is also evident. Figure 3 illustrates the loss rate on a linear scale as it would be detected by a beam-loss monitor. The (small) degree of left-right asymmetry changes with the mass of the macroparticle.

The dependence of the peak loss rate on macroparticle mass and total proton intensity is further illustrated for an

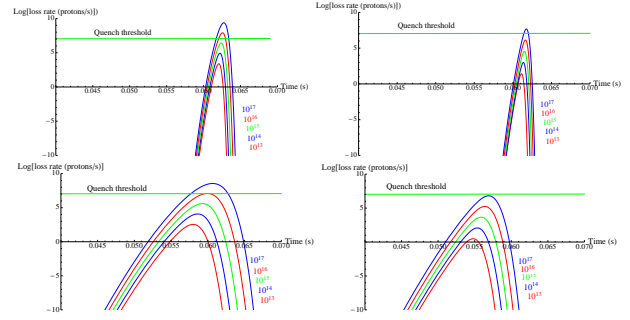


Figure 2: Beam loss rate as a function of time at 10% of the design current (left) and twice the design current (right) for an rms beam size of 0.3 mm (top) and 1.2 mm (bottom).

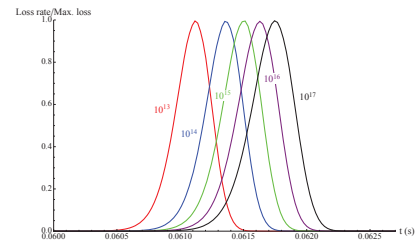


Figure 3: Normalized loss rate on a linear scale as a function of time for different macroparticle masses, with an rms beam size of 0.3 mm and a proton intensity of 1.6×10^{14} .

rms beam size of 0.3 mm by Fig. 4. A certain structure is seen. Figure 5 depicting the peak loss rate as a function of rms beam size for different macroparticle masses A reveals a similar pattern. The local peaks in the loss rate have been found to correlate with peaks in the final macroparticle charge.

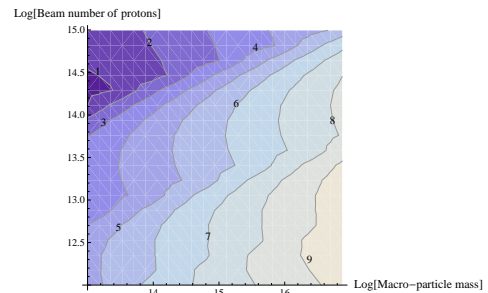


Figure 4: Contour plot of maximum loss rate (on log scale; numbers indicate $\log_{10} \dot{N}_{\text{lost}}$ where \dot{N}_{lost} is in units of protons per second) as a function of macroparticle mass and total number of protons (also both on log scale) for an rms beam size of 0.3 mm.

The next two figures illustrate the loss duration defined as the time interval in which the loss rate exceeds 1 p/s, Fig. 6 as a function of rms beam size, and Fig. 7 as a function of total proton intensity. The loss duration scales linearly with the beam size, increases weakly with the macroparticle mass, and above 10^{12} protons decreases with the beam intensity.

Finally, we look at the total number of lost protons, i.e. the integral of the loss rate over time. Figure 8 presents this as a function of macroparticle mass and total intensity

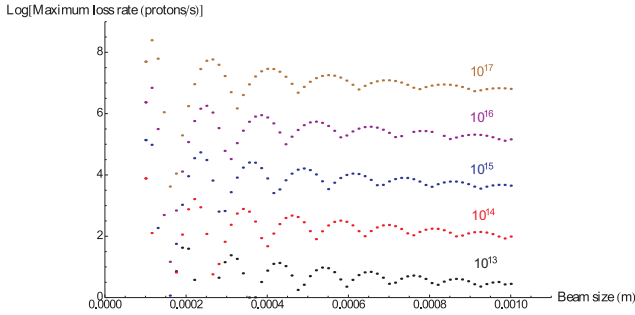


Figure 5: Maximum loss rate as a function of rms beam size for different macroparticle masses as indicated and a total beam intensity of 6.5×10^{14} .

for a fixed beam size of 0.3 mm. The number of lost protons has a maximum as a function of beam intensity and is highest for about 10^{13} protons. Figure 9 shows the total number of lost protons as a function of macroparticle mass and rms beam size, both on a linear and on a logarithmic scale. The loss is highest for an rms beam size of 0.2 mm.

The loss duration is almost independent of the material; the total losses are weakly dependent, e.g. for copper instead of aluminium about 20% less protons are lost [8].

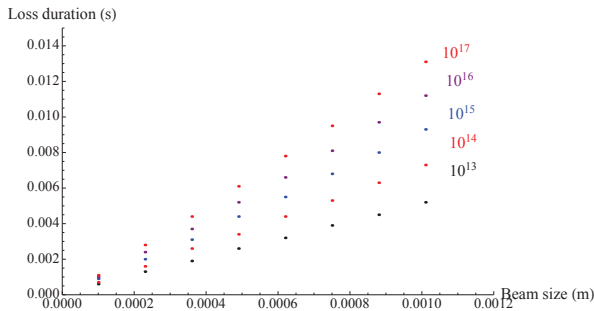


Figure 6: Loss duration as a function of rms beam size for a beam intensity of 3.2×10^{13} .

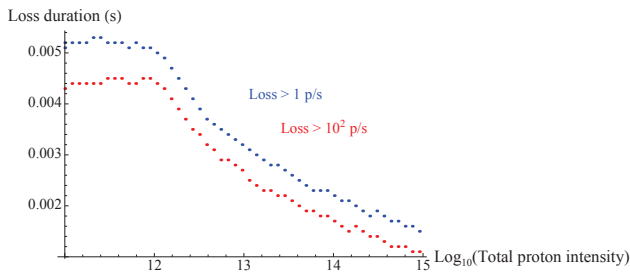


Figure 7: Loss duration as a function of total beam intensity for an rms beam size of 0.3 mm and a macroparticle mass $A = 10^{15}$.

CONCLUSIONS

The model of a fallen macroparticle makes several predictions consistent with LHC UFO observations [2, 3]: (1) Sufficiently heavy macroparticles give rise to a maximum beam loss rate at or above the quench threshold. (2) The loss time duration is of order 1 ms. (3) The computed loss duration is constant up to an intensity of 10^{12} protons and then gets shorter for increasing beam current.

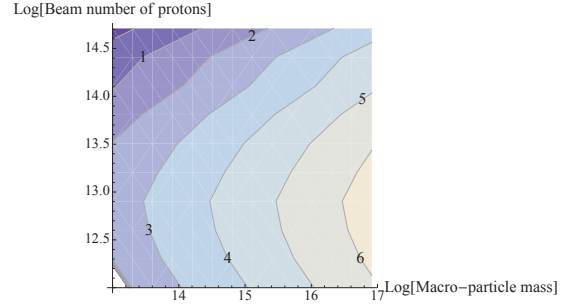


Figure 8: Contour plot of total number of lost protons N_{lost} (on log scale; numbers indicate $\log_{10}(N_{\text{lost}})$) as a function of macroparticle mass and beam intensity (both on log scale as well) for an rms beam size of 0.3 mm.

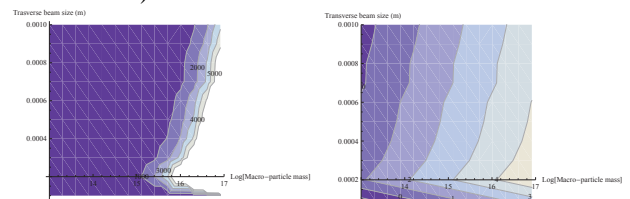


Figure 9: Contour plot of total number of lost protons as a function of macroparticle mass (on log scale) and transverse beam size at the LHC design intensity (3.2×10^{14}): linear scale for lost protons [numbers] (left), and log scale (right).

Further model predictions are as follows: (4) The total number of lost protons is maximum for a total proton beam intensity of 10^{13} and decreases with higher intensity, roughly in inverse proportion. (5) For decreasing beam size the peak loss rate increases while the loss duration decreases. The total number of lost protons shows a non-monotonic dependence on the beam size: it is maximum at a beam size of about $200 \mu\text{m}$, a typical value for the LHC arcs at top energy. Increasing the beam size by a factor of 5 reduces the total number of lost protons by about a factor of 3. (6) The time separation between a first and a second crossing predicted by the model is consistent with some occasional beam observations of multiple successive events.

In the future we plan to revise the equation for the macroparticle charging rate, to model its temperature, to investigate the effect of an electron cloud on the macroparticle charge state and trajectory evolution, and to look at other than spherical objects.

REFERENCES

- [1] M. Sapinski et al, Proc. Chamonix LHC Performance Workshop 2011, CERN-2011-005, p. 209–214.
- [2] E. del Busto et al, “Analysis of Fast Losses in the LHC with the BLM System,” IPAC 2011 San Sebastian.
- [3] T. Baer et al, “UFOs in the LHC,” IPAC 2011 San Sebastian.
- [4] M. Giovannozzi et al, Proc. IPAC’10 Kyoto (2010).
- [5] F. Zimmermann, DESY HERA 93-08 (1993).
- [6] Wolfram Research, Mathematica 7.
- [7] M. Brugger et al., CERN-AB-Note-2007-018 ATB (2007).
- [8] Z. Yang, TP IVb report, EPFL Lausanne, June 2011.